

RESEARCH ARTICLE

Jaw morphology and fighting forces in stag beetles

Jana Goyens^{1,2,*}, Joris Dirckx² and Peter Aerts^{1,3}

ABSTRACT

The jaws of different species of stag beetles show a large variety of shapes and sizes. The male jaws are used as weapons in fights, and they may exert a very forceful bite in some species. We investigated in 16 species whether and how the forcefulness of their bite is reflected in their jaw morphology. We found a large range of maximal muscle forces (1.8–33 N; factor of 18). Species investing in large bite muscles also have disproportionately large jaw volumes. They use this additional jaw volume to elongate their jaws, increasing their chances of winning in battles. The fact that this also decreases the mechanical advantage is largely compensated for by elongated levers. As a result, high muscle forces are correlated with elevated bite forces (0.27–7.6 N; factor of 28). Despite the large difference in the forcefulness of their bite, all investigated species experience similar Von Mises stresses in their jaws while biting (29–114 MPa; factor of 4.0; calculated with finite element simulations). Hence, stag beetles have successfully adapted their jaw anatomy according to their bite force in fights.

KEY WORDS: Lucanidae, Finite element analysis, Bite force, Animal weaponry, Mechanical advantage, Jaw length

INTRODUCTION

Animal weapons often show a high morphological diversity. This is exemplified by the jaws of stag beetles, the antlers of cervids and the horns of bovids and beetles. The diversification of beetle horns was probably stimulated by the different costs horns pose depending on the species' ecology. For example, horns at the front of the head are rare in nocturnal species because they are correlated with smaller eyes and, therefore, reduced vision (Emlen, 2001). However, for most families, it remains unknown what exactly caused this evolutionary diversification (Emlen, 2008), and an in-depth understanding of the functional morphology of these weapons is essential to gain insight into this process. Stag beetles (family Lucanidae) are an interesting model animal in this regard. Not only do they display a remarkable diversity in the size and shape of male weapons (varying from small, indistinct jaws to impressive jaws that are longer than the rest of the body; see Fig. 1) but also their bite forces are probably equally diverse (considering the range of head sizes; see Fig. 1). Hence, the stag beetle family may comprise an interesting range of different morphological strategies. Depending on their specific fight behaviour, species may need long jaws or jaws with a specific shape. Furthermore, they may have invested in

large and heavy musculature to bite their rivals forcefully. Concomitantly, species with high bite forces probably needed to evolve a more robust jaw morphology to enable them to take a firm grip on rivals and to avoid mechanical failure (Goyens et al., 2015a).

In sexually dimorphic stag beetle species, males with larger jaws have higher mating rates than males with smaller jaws (Harvey and Gange, 2006; Lagarde et al., 2005; Okada and Hasegawa, 2005; Okada and Miyatake, 2006; Shiokawa and Iwahashi, 2000). Owing to their longer jaws, they can reach further forward in aggressive battles to grab their opponent and to detach him from the substrate (Goyens et al., 2015b). Once detached, the opponent is pushed away or lifted above the winner's head and thrown backwards onto the substrate (Goyens et al., 2015b; Shiokawa and Iwahashi, 2000). In addition to the stag beetles' jaws being elongated, their enlarged jaw-closer muscles enable high bite forces (Goyens et al., 2014a; Shiokawa and Iwahashi, 2000). In turn, these high bite forces probably require jaws that are robust against bending (Goyens et al., 2014b,c). However, these adaptations of stag beetle weaponry come at a cost. First, there are the direct locomotion costs of running and flying with heavy weapons (the energy cost increases by 38% and 26%, respectively, in *Cyclommatus metallifer* males compared with females of the same species; Goyens et al., 2015d,e). Second, stag beetles are holometabolous insects, and the growing mandibles have to compete with other body parts for resources in the pupa (Kawano, 1997; Knell et al., 2004).

In this study, we compared the weapon morphology of 16 stag beetle species with a wide range of jaw anatomies and associated muscle sizes (see Fig. 1). By combining finite element (FE) analysis with measurements of bite muscle size, we examined whether and how the jaw morphology of these 16 species is adapted to withstand deformations while biting. We hypothesized that stag beetles have adapted their jaw morphology according to their bite force, and that this prevents elevated material stresses that might cause structural failure in the jaws of species with a more forceful bite.

MATERIALS AND METHODS

Micro-computed tomography (CT) scans

We obtained adult male stag beetles of 16 species from nine different genera, with a large variety of jaw sizes and shapes (see Fig. 1): *Cyclommatus lunifer* Boileau 1905 (specimen 1), *Cyclommatus metallifer* (Boisduval 1835) (specimen 2a), *Dorcus alcidis* Vollenhoven 1865 (specimen 3), *Dorcus bucephalus* (MacLeay 1819) (specimen 4), *Dorcus parryi* (Boileau 1902) (specimen 5), *Dorcus titanus* (Boisduval 1835) (specimen 6), *Hexarthrus parryi* Hope 1842 (specimen 7), *Lamprima adolphinae* (Gestro 1875) (specimen 8), *Lucanus cervus* (Linnaeus 1758) (specimen 9), *Nigidius obesus* Parry 1864 (specimen 10), *Prismognathus davidis* Deyrolle 1878 (specimen 11), *Prosopocoilus bison* (Olivier 1789) (specimen 12), *Prosopocoilus giraffa* Olivier 1789 (specimen 13), *Prosopocoilus mohnikei* Parry 1873 (specimen 14), *Prosopocoilus senegalensis* (Latreille 1817) (specimen 15) and *Pseudorhaetus oberthuri* Planet 1899

¹University of Antwerp, Laboratory of Functional Morphology, Universiteitsplein 1, Antwerp 2610, Belgium. ²University of Antwerp, Laboratory of Biophysics and BioMedical Physics, Groenenborgerlaan 171, Antwerp 2020, Belgium. ³Ghent University, Department of Movement and Sport Sciences, Watersportlaan 2, Ghent 2000, Belgium.

*Author for correspondence (jana.goyens@uantwerpen.be)

 J.G., 0000-0003-0176-884X



Fig. 1. Pictures of the heads of the stag beetle specimens used in this study. All specimens are male beetles of a different species, except for specimen 2b. All photos are shown at the same magnification. The scale bar indicates 5 mm.

(specimen 16). Further, we acquired a female *C. metallifer* individual (specimen 2b). All specimens were purchased from authorized commercial dealers (The Pet Factory Germany, www.thepetfactory.de; The Bugmaniac, www.thebugmaniac.com; Kingdom of Beetle Taiwan, screw-wholesale.myweb.hinet.net), except for the dead specimen of *L. cervus*, which was collected in France [collaboration with Research Institute for Nature and Forest (INBO), permission reference BL/FF-SB 09-03188]. These species are not listed on CITES appendices (checklist.cites.org). Except for the *L. cervus* and *C. metallifer* specimens, all specimens were dried. Because we only used the morphology of the exoskeleton in our analyses, our results are not affected by shrinkage of soft tissue because of drying. We made micro-CT scans of the male specimens with a Skyscan 1172 high resolution micro-CT scanner (Bruker micro-CT, Kontich, Belgium). The female specimen was scanned by the Centre for X-ray Tomography of Ghent University. The micro-CT scanners were operated at voltages of 59–120 kV and currents of 117–200 μ A, which resulted in a resolution of 11–13 μ m.

Bite muscles

Ross et al. (2005) demonstrated that muscle forces can be applied in FE analyses by estimating their overall force amplitude from the physiological cross-sectional area (PCSA) of the muscle (Ross et al., 2005). For stag beetle bite muscles (i.e. closer muscles of the jaws), the PCSA can be approximated by examining the attachment area of the muscles on the head (Goyens et al., 2014a). The closer muscles diverge from the jaw to the head capsule and have the shape of a 3D cone (Goyens et al., 2014a). In *C. metallifer*, males have a very large fighting apparatus and head, while females have small, indistinct jaws and head. Despite this large sexual difference, the head is almost completely filled with bite muscles in both sexes (Goyens et al., 2014a), and the ratio of head surface area to muscle attachment surface is almost identical (males: 35%, females: 34%). As a result, we could estimate the PCSA of all specimens using the external head surface (excluding the mandibles and other mouth parts). This estimation was necessary because the muscle attachment area on the head was often not visible on scans of the dried samples. The external head surface area is very similar to the internal head surface area (because of the relatively thin head exoskeleton), but measuring the latter induces more artefacts due to the remains of soft tissue inside the head. We determined the external head surface area of the 16 species using the 3D image processing software Amira (v. 5.4.4; 64-bit version, FEI, Hillsboro, OR, USA). First, we determined which voxels belong to the head with a combination of automatic grey-scale thresholding and manual corrections in the three orthogonal views. Second, we

created and smoothed out a triangulated surface mesh of the head and calculated its area. Using this head surface area, we calculated the muscle force with the muscle stress (muscle force per PCSA) that was previously determined for *C. metallifer* stag beetles (Goyens et al., 2014a). This assumes that all species are capable of developing the same maximal muscle stress, which is a reasonable assumption because muscle stress in *C. metallifer* males is almost identical to that of females (which are not adapted for fighting; 18 and 17 N cm^{-2} , respectively; Goyens et al., 2014a).

FE simulations of jaw biting

The FE method is a numerical method that can be used for the structural analysis of (complex) loaded structures. These structures are subdivided into a large number of small elements (a mesh), for which stresses (Von Mises stresses), strains and displacements are calculated (Bright, 2014; Dumont et al., 2009; Rayfield, 2007).

Using the same method that we used to create the surface meshes of the heads, we also made surface models of the jaw cuticle for all 16 species. Based on these surface models, we calculated jaw cuticle volume, jaw length (out-lever, hinge–jaw tip) and input lever arm length (in-lever, hinge–muscle attachment on jaw; see Fig. 2) in Amira. By multiplying the muscle force by the mechanical advantage (in-lever divided by jaw length), we estimated the specimens' bite forces (Goyens et al., 2014a; Mills et al., 2016). We established scaling relationships between morphological variables after log–log transformation with the reduced major axis. The measured slope was considered to be significantly different from the slope predicted by isometry if the latter fell outside the 95% confidence interval (Moran, 1971; Smith, 2009).

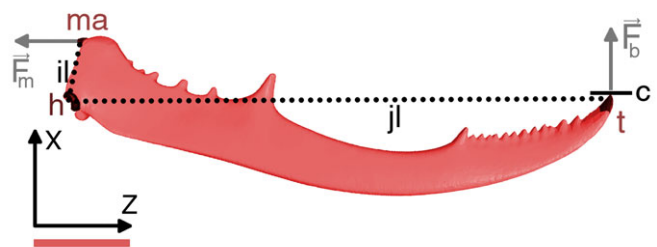


Fig. 2. Overview of the finite element (FE) model. The tip (t), hinge (h) and bite muscle attachment (ma) are indicated with darker areas on the 3D model of the male *Cyclommatus metallifer* jaw. Dotted lines show the in-lever length (il) and the jaw length (jl). Movement in x-direction of the jaw tip is constrained (c). The muscle force (F_m) and the bite force (F_b) that it elicits are shown (drawn with arbitrary vector lengths). The scale bar indicates 5 mm.

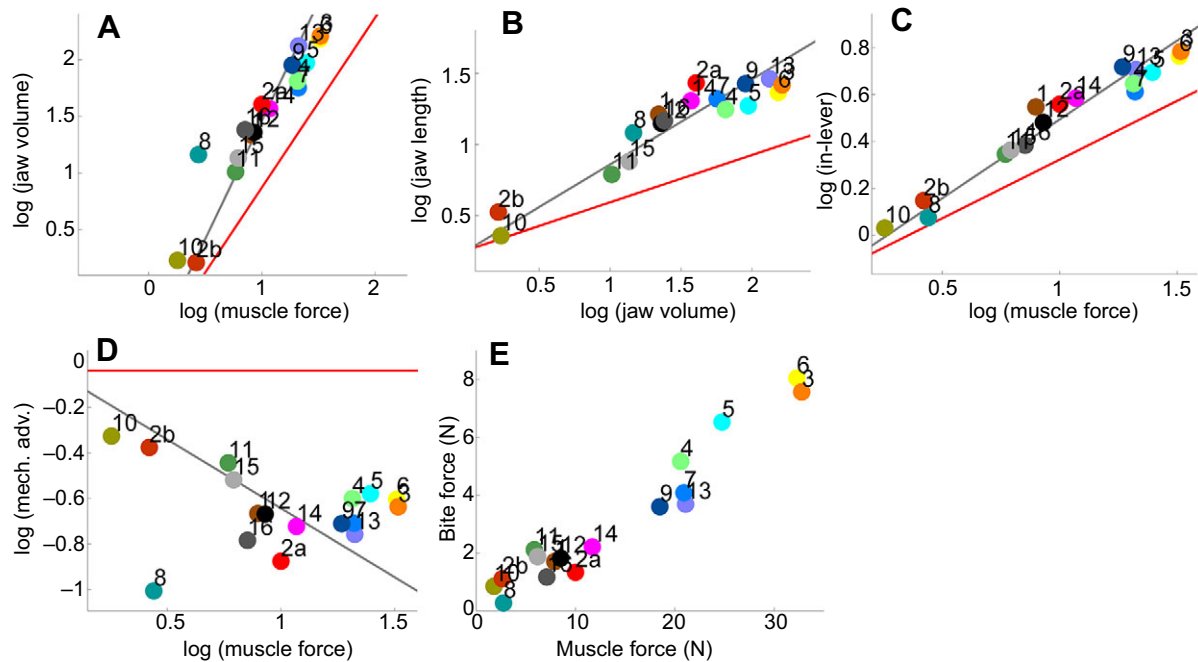


Fig. 3. Correlations between morphological jaw parameters. Correlations are shown for muscle force (calculated using head surface area), jaw volume (cuticle volume), jaw length (out-lever), in-lever length, mechanical advantage and bite force. The grey line shows the fitted slope, the red line shows the slope predicted under isometry.

Starting from the surface model, we subsequently made a tetrahedral volume mesh with TetGen software (v. 1.4. tetgen.org). Each model contained at least as many tetrahedral elements as determined for a *C. metallifer* model by a convergence analysis (Rayfield, 2007). We then made separate FE simulations with each of these 3D jaw volume models in FEBio (FEBio v. 1.4.1; Maas et al., 2012). The jaw material was modelled to be linearly elastic and isotropic, with a Young's modulus of 5.1 GPa and a Poisson ratio of 0.3. These material properties are the same as those measured for *C. metallifer* (Goyens et al., 2014b). The FE model of *C. metallifer* was previously successfully validated with an experimental measurement of the jaw deformation during biting using an optical technique (digital image correlation; Goyens et al., 2014b). This ensures that the model accurately reproduces the biological reality (Bright, 2014; Rayfield, 2007). For a detailed description of the model and its validation, see Goyens et al. (2014b). A muscle force was applied at the muscle attachment site, which caused a moment about the jaw hinge. The jaw hinge motion was constrained, so that it did not translate, and only rotated about its hinge axis. We constrained movement in the *x*-direction of the most distal tip of the jaw (i.e. the direction of the bite force; see Fig. 2), to mimic the biting of an opponent. All boundary conditions (i.e. the hinge, muscle attachment and bite point) were applied to a group of elements, rather than a single node, to reduce artefacts (see Fig. 2). Using FE routines, we calculated Von Mises stresses during biting, which predict the failure of ductile materials (Rayfield, 2007). From the material stress results of our FE models, we removed the high value singularities, to avoid interpreting artefacts (Dumont et al., 2005). We used distance-based outlier detection for this purpose (a proximity-based approach; Knorr and Ng, 1997); elements are considered to be outliers if there are less than *X* elements (percentage π ; 0.0025% of the total number of elements) with an approximately equally high material stress (radius ϵ ; 10 MPa). We made three sets of FE simulations, each with different input forces, as described below.

In the first set of FE simulations (the 'natural loading' simulations), we implemented the real muscle force for each species, based upon calculations of the head surface area (see 'Bite muscles', above).

In the second set of FE simulations (the 'same size' simulations), the input force was scaled for the difference in surface area of the jaw models, to account for the size variation of the jaws (Dumont et al., 2009).

In the third set of FE simulations (the 'same jaw CSA' simulations), we scaled the input force in the FE simulations according to the average cross-sectional area of the jaw (jaw CSA; jaw cuticle volume divided by jaw length). This corrects (1) for the fact that some species invest in more exoskeletal material (a higher jaw volume) and (2) that species may use the additional jaw volume to increase their jaw length disproportionately (rather than increasing their jaw robustness). Differences in maximal material stress result purely from differences in jaw shape.

The input forces of all models, as well as the number of elements, are given in Table S1.

RESULTS

Morphological scaling

The muscle forces of the investigated specimens range from 1.8 to 33 N (18-fold difference), which results in bite forces from 0.27 to 7.6 N (28-fold difference). Jaw volume and in-lever length both show a strong positive allometry with muscle force (as defined by head surface area; see Fig. 3A,C, Table 1). Both increase faster with increasing muscle force than predicted under isometry (the slope predicted under isometry falls outside the 95% confidence interval). Also, jaw length increases faster with increasing jaw volume than predicted under isometry (see Fig. 3B, Table 1). In contrast, the mechanical advantage decreases with increasing muscle force, while under isometry, this would have remained constant (see Fig. 3D, Table 1). Nevertheless, there exists a strong positive relationship between muscle force and bite force (see Fig. 3E, Table 2).

Table 1. Correlations between morphological variables

Figure	Fitted slope	Predicted slope	CI
3A	0.67	1/2	0.59; 0.76
3B	2.1	3/2	1.8; 2.4
3C	0.60	1/3	0.50; 0.72
3D	−0.60	0	−1.36; −0.24

The corresponding figure, the fitted slope between the variables and its confidence interval (CI) are given. The slope that was predicted under isometry never lies within the CI, indicating that the actual slope is significantly different.

FE simulations

Fig. 4 shows the material stress distribution in the ‘natural loading’ simulations. The region with the highest stress has the highest potential for structural failure (Dumont et al., 2009), although exceptions may occur as a result of individual variation, material fatigue, etc. The location and amplitude of the maximal material stress differ between specimens. For example, for the *C. lunifer* (specimen 1) and *P. bison* (specimen 12) specimens, the maximal material stress is located near the jaw tip. Therefore, they would probably only lose the tip of their jaws through overloading. However, other specimens, such as *D. alcides* (specimen 3) and *P. mohnikaei* (specimen 14), are likely to lose their entire jaw when the ultimate material stress is reached, because the maximal material stress is located near their jaw base. The amplitude of the maximal material stress is independent of the maximal muscle force under natural loading (see Fig. 5A) and also when the effect of jaw size is excluded (see Fig. 5B). A comparison of linear mixed models that take genus into account indeed fails to reject the hypothesis that the slope equals zero (see Table 2). Hence, the jaws of species with elevated muscle forces are robust enough to prevent an increased material stress.

In the ‘same jaw CSA’ simulations, differences in material stress are due to jaw shape variation (see Fig. 5C). Most species have a similar, low, material stress (<100 MPa; see Fig. 5C). Again, a comparison of linear mixed models that take the genus into account fails to reject the hypothesis that the slope equals zero (see Table 2). However, some species have substantially higher material stresses. Except for the *L. cervus* specimen (specimen 9), species with such delicate, non-robust jaw shapes do not bite forcefully.

DISCUSSION

The stag beetle family Lucanidae contains a very large diversity of weapon sizes and shapes which are associated with a large range of bite muscle forces. We found that the two are interrelated. Species with large, strong bite muscles have robust jaw shapes, preventing their high bite forces from increasing the risk of structural failure. Further, they have disproportionately long jaws, which enhance their chances of winning in battles. These long out-levers decrease

Table 2. Statistical comparison between linear mixed models of the correlation between a dependent variable (bite force or material stress) and muscle force, and a linear model with a slope of zero

Figure	Set of FE simulations	χ^2	P-value
3E	–	34	<0.0001
5A	‘Natural loading’	0.068	0.79
5B	‘Same size’	1.7	0.19
5C	‘Same jaw CSA’	1.9	0.17

The genus of the species is taken into account as a random factor. The χ^2 and P-value are given for the ANOVA that compares the two linear models. FE, finite element.

the mechanical advantage, but this effect is largely compensated for by elongated in-levers.

Morphological adaptations

We found a very broad range of muscle forces in the stag beetle family (factor of 18). If this were the result of isometric growth of the head (including the jaws), isometric relationships would exist between parameters that describe head and jaw size. We found that this is not the case. Jaw volume increases faster with increasing muscle force (which is related to head surface area) than predicted under isometry (see Fig. 3A). This investment in jaw volume (material, weight) is used to elongate the jaw length disproportionately (see Fig. 3B). This agrees with the observation that in several stag beetle species, males with the longest jaws are more likely to win battles (Goyens et al., 2015b; Inoue and Hasegawa, 2012; Lagarde et al., 2005; Mills et al., 2016), probably owing to a longer reach to the rival’s legs when trying to dislodge it from the substrate (Goyens et al., 2015b). Also, the in-lever grows disproportionately fast with increasing muscle force (Fig. 3C), but not fast enough to compensate entirely for the increased out-lever because of jaw elongation. As a result, the mechanical advantage is lower in specimens with larger bite muscles (Fig. 3D). This partly negates the effect of the enlarged bite muscles but, nevertheless, bite force is strongly related to muscle force and a large range of bite forces is observed (factor of 28; see Fig. 3E).

Mechanical robustness

The scaling analysis indicates that males with stronger bite muscles use their larger jaw volume to increase their jaw length disproportionately. Our FE simulations show that this does not come at the detriment of jaw robustness. Forceful biters undergo material stresses that are similar to those of weak biters and females (see Fig. 5A,B). This shows that the investigated males with a forceful bite have adapted their jaw morphology to their bite force, in order to prevent an increased material stress and failure risk. FE analyses have also shown a functional adaptation of the robustness of scorpion chelae; sand-dwelling species have slender, elongated chelae, while species that burrow or feed on hard prey have robust chelae with short fingers (van der Meijden et al., 2012). However, contrary to our results on stag beetles, scorpions with slender chelae still have to bear higher Von Mises stresses, despite their lower pinch force (van der Meijden et al., 2012). In both Darwin’s finch beaks and rhinoceros horns, structural adaptations ensure lower Von Mises stresses during natural (typical) loading conditions than during atypical loadings (McCullough et al., 2014; Soons et al., 2015). Nevertheless, FE analyses revealed that this does not prevent rhinoceros beetle species experiencing substantially different maximal natural material stresses (McCullough et al., 2014). In battles, stag beetle jaws also undergo additional loadings when lifting their rivals. However, accelerations measured from high-speed video recordings of fighting *C. metallifer* males (J.G., unpublished results) show that these dorso-ventral forces are very small compared with the bite forces. Concomitantly, their jaws are more resistant to bending caused by biting than by dorso-ventral loadings (Goyens et al., 2015a).

Our FE analyses of the *H. parryi* (specimen 7) and *L. cervus* (specimen 9) specimens show high material stresses under natural loading conditions (see Fig. 5A). Nevertheless, they do engage in combat (*H. parryi*: J.G., personal observations; *L. cervus*: Fremlin, 2009; Percy, 1998), but they may not bite with the most distal tip of their jaws. For example, *L. cervus* often bites with the medial ‘tooth’ on the jaw. This results in much lower material stresses in the

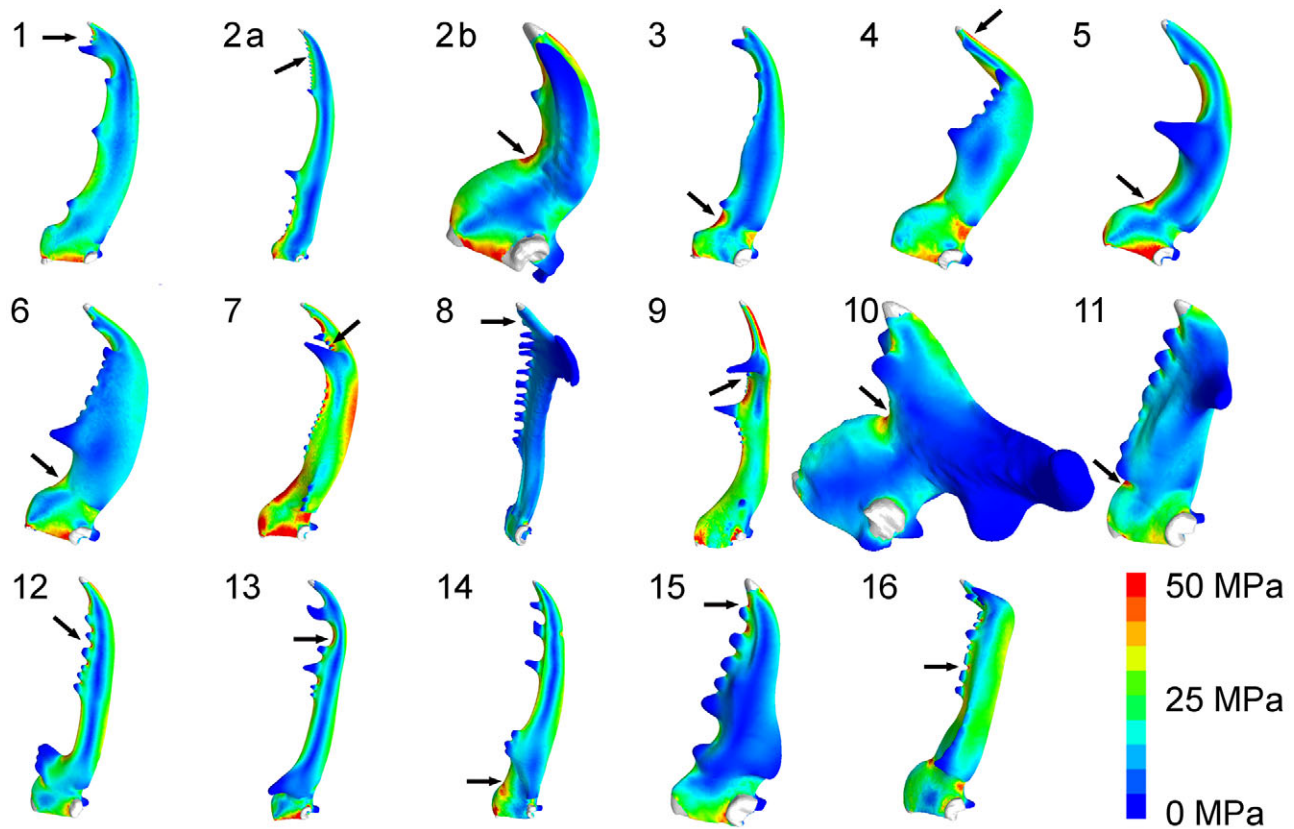


Fig. 4. Comparison of Von Mises stress distribution on the dorsal jaw surface, calculated using the ‘natural loading’ simulations. For visualization purposes, the jaws are depicted with the same jaw length. Arrows indicate the location of maximal material stress.

simulations, which are not outliers in Fig. 5 (material stresses of 59, 48 and 73 MPa in Fig. 5A–C, respectively). Alternatively, they may reduce their failure risk by modulating their bite muscle force (as *C. metallifer* is capable of doing; Goyens et al., 2014b) or by enhanced material properties. Further, it can of course not be excluded that our assumptions regarding the size and stress of the bite muscles are less appropriate for these species.

Fighting strategies

There is little in the scientific literature about interspecific variation in fighting strategies and methods of stag beetles (Goyens et al., 2015b). Our results may predict the importance of aggressive

fighting in the mating behaviour of stag beetles. Some of the investigated specimens show a large investment in bite musculature, combined with morphological adaptations of the jaws (i.e. in-lever length and jaw length; see above). It can be assumed that they use these properties in aggressive encounters. In contrast, specimens with low muscle forces probably do not use their jaws in aggressive fights and consequently they were observed to have delicate jaw shapes [see Fig. 5C; material stress >100 MPa and muscle force <9 N; except for *L. cervus* (specimen 9), but see above]. The other examined specimens have similar, lower, material stresses (between 63 and 93 MPa), despite their large range of muscle forces. Hence, their jaw shape, despite being very different, is approximately

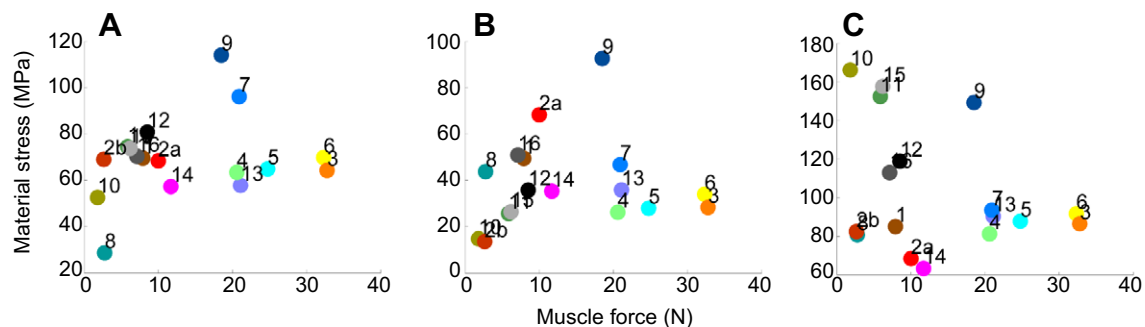


Fig. 5. Correlation between muscle force and Von Mises stress. (A) The ‘natural loading’ simulations. (B) The ‘same size’ simulations. (C) The ‘same jaw CSA’ simulations. In A and B, the maximal value of the material stress does not increase with muscle force for most specimens. In C, the jaw shape of a number of specimens results in a similar, low, material stress despite the large difference in muscle force. CSA, cross-sectional area.

equally good from a mechanical point of view. Also, the horn robustness of bovids and cervids is adapted to their fighting style. For example, in bovids that typically use their horns for ramming (such as bighorn sheep and African buffalos), the horns are a lot more massive and recurved than those of bovid species that stab, wrestle or fence with their horns (Lundrigan, 1996).

Weapon morphology – functional amplification or many-to-one mapping

High bite forces in stag beetle species are realized by a combination of in-lever elongation and bite muscle enlargement (see Fig. 3C). Such functional amplification (different morphological changes evolve congruently to enhance the same function) was also found in mantis shrimps; in ‘smashers’, the lever system and the linkage system evolved together towards force maximization, while in ‘speakers’, both systems are adapted for speed maximization (Anderson et al., 2014). Such correlated evolution points to a relatively restricted evolutionary pattern, as opposed to many-to-one mapping (in which different combinations of morphologies result in the same mechanical output; Anderson et al., 2014; Wainwright et al., 2005; Young et al., 2007). Nevertheless, stag beetles show a remarkable diversity in weapon shapes. The question remains, though, as to why this is the case. With more similar jaw shapes, they could also have stayed within a narrow range of material stresses. Jaw shape diversity is probably stimulated by its relatively low cost (Goyens et al., 2015d), possibly combined with volatile selective pressures, the advantages of novel weaponry features and/or habitat-specific modifications (for a review, see Emlen, 2008).

Material properties

Scientific knowledge about biomechanical and morphological properties of stag beetle weapons is even more scarce than literature on their phylogeny. The size and stress of the bite muscle and the Young’s modulus of the jaw exoskeleton are only known for *C. metallifer* (Goyens et al., 2014b). Based on the finding that these properties do not differ between sexes (i.e. they are not adapted in *C. metallifer* males), we assumed that they were similar in all species under investigation. Future experiments may confirm or reject this assumption. Because our FE simulations show that such adaptations are not required to avoid an elevated failure risk, we hypothesize that these properties are similar within the investigated species. If true, this may also have stimulated the high diversity in weapon shapes and bite forces within the stag beetle family (see section ‘Weapon morphology’, above).

Male stag beetles fight repeatedly in their adult life stage, which may cause scratches and other kinds of damage on the mandibles. Such wear may increase the failure risk, for example by notch propagation. It is not yet known how this influences the toughness of the mandibles, and whether their material properties are adapted to prevent an increased failure risk. Stag beetle mandibles consist of sclerotized, reinforced cuticle (Cribb et al., 2010; Goyens et al., 2014b; Klocke, 2011; Vincent and Wegst, 2004). As a result, aggressive fighting and biting probably cause only superficial scratches, as seen under a scanning electron microscope (Goyens et al., 2014b). This suggests that the (adult) age of stag beetles hardly influences their failure risk. The claws of *Cancer* crabs, in contrast, are known to suffer from wear and fatigue. Later instars compensate for this by behaviourally reducing their muscle stress (Taylor, 2000).

Phylogenetic considerations

Despite substantial scientific interest in the stag beetle family, the phylogeny of this large family (counting more than 1000 species)

remains largely unknown (Hosoya and Araya, 2005; Kawano, 2000; Kim and Farrell, 2015). Therefore, a fully phylogenetically corrected statistical analysis (e.g. Felsenstein’s method of independent contrasts or generalized least squares; Taylor and Thomas, 2014) is not yet possible. However, we did correct for the fact that some of the investigated species belong to the same genus with linear mixed models. Also, a graphical comparison shows that the genera with several species under investigation follow the same trend as the complete dataset (see Fig. S1), which qualitatively suggests that the phylogenetic error covariance is low.

Individual variation

We investigated 16 specimens, each of a different stag beetle species. Some stag beetle species are known to exhibit a large variability in jaw sizes and sometimes also jaw morphologies (Kawano, 2000; Rowland and Emlen, 2009). In some stag beetle species, the relationship between body size and mandible length is non-linear, and jaw dimorphism and trimorphism occur in the family (Emlen and Nijhout, 2000; Rowland and Emlen, 2009). The existence of multiple male morphs in some species does not compromise the present aims and results. We did not aim to draw species-wide conclusions, but rather we searched for evolutionary trends throughout the family. While some of the investigated species may also have a smaller (minor) morph, our simulations show that the jaws of the larger conspecifics with a more forceful bite are robust enough to safely withstand their bites.

Acknowledgements

The authors thank Manuel Dierick of UGCT (Ghent University, Belgium) for providing the micro-CT reconstructions of the female jaw; Arno Thomaes of INBO for the *Lucanus cervus* specimen, for inspiring discussions and for suggesting interesting literature; and Josie Meaney for proofreading the manuscript before submission.

Competing interests

The authors declare no competing or financial interests.

Author contributions

J.G. executed the micro-CT scans of the male specimens, ran the FE simulations and drafted the article. J.G., J.D. and P.A. analysed and interpreted the findings and revised the article.

Funding

This study was supported by a Bijzonder Onderzoeksfonds grant (IDBOFUA 2011-445-a) of the Research Council of the University of Antwerp. The SkyScan1172 high-resolution micro-CT scanner, located at the VUB facilities, was funded by the Hercules Foundation (Herculesstichting, grant no. UABR/ 11/004).

Supplementary information

Supplementary information available online at <http://jeb.biologists.org/lookup/doi/10.1242/jeb.141614.supplemental>

References

- Anderson, P. S. L., Claverie, T. and Patek, S. N. (2014). Levers and linkages: mechanical trade-offs in a power-amplified system. *Evolution* **68**, 1919–1933.
- Bright, J. A. (2014). A review of paleontological finite element models and their validity. *J. Paleontol.* **88**, 760–769.
- Cribb, B. W., Lin, C.-L., Rintoul, L., Rasch, R., Hasenpusch, J. and Huang, H. (2010). Hardness in arthropod exoskeletons in the absence of transition metals. *Acta Biomater.* **6**, 3152–3156.
- Dumont, E. R., Piccirillo, J. and Grosse, I. R. (2005). Finite-element analysis of biting behavior and bone stress in the facial skeletons of bats. *Anat. Rec. A* **283**, 319–330.
- Dumont, E. R., Grosse, I. R. and Slater, G. J. (2009). Requirements for comparing the performance of finite element models of biological structures. *J. Theor. Biol.* **256**, 96–103.
- Emlen, D. J. (2001). Costs and the diversification of exaggerated animal structures. *Science* **291**, 1534–1536.
- Emlen, D. J. (2008). The evolution of animal weapons. *Annu. Rev. Ecol. Evol. Syst.* **39**, 387–413.

- Emlen, D. J. and Nijhout, H. F.** (2000). The Development and Evolution of exaggerated morphologies in insects. *Annu. Rev. Entomol.* **45**, 661–708.
- Fremlin, M.** (2009). Stag beetle (*Lucanus cervus*, (L., 1758), Lucanidae) urban behaviour. In Proceedings of the 5th Symposium and Workshop on the Conservation of Saproxylic Beetles, pp. 161–176.
- Goyens, J., Dirckx, J., Dierck, M., Van Hoorebeke, L. and Aerts, P.** (2014a). Biomechanical determinants of bite force dimorphism in *Cyclommatus metallifer* stag beetles. *J. Exp. Biol.* **217**, 1065–1071.
- Goyens, J., Soons, J., Aerts, P. and Dirckx, J.** (2014b). Finite Element modelling reveals force modulation of jaw adductors in stag beetles. *J. R. Soc. Interface* **11**, 20140908.
- Goyens, J., Dirckx, J., Piessen, M. and Aerts, P.** (2015a). Role of stag beetle jaw bending and torsion in grip on rivals. *J. R. Soc. Interface* **13**, 20150768.
- Goyens, J., Dirckx, J. and Aerts, P.** (2015b). Stag beetle battle behaviour and its associated anatomical adaptations. *J. Insect Behav.* **28**, 227–244.
- Goyens, J., Dirckx, J. and Aerts, P.** (2015c). Built to fight: variable loading conditions and stress distribution in stag beetle jaws. *Bioinspir. Biomim.* **10**, 046006.
- Goyens, J., Van Wassenbergh, S., Dirckx, J. and Aerts, P.** (2015d). Cost of flight and the evolution of stag beetle weaponry. *J. R. Soc. Interface* **12**, 20150222.
- Goyens, J., Dirckx, J. and Aerts, P.** (2015e). Costly sexual dimorphism in *Cyclommatus metallifer* stag beetles. *Funct. Ecol.* **29**, 35–43.
- Harvey, D. J. and Gange, A. C.** (2006). Size variation and mating success in the stag beetle *Lucanus cervus*. *Physiol. Entomol.* **31**, 218–226.
- Hosoya, T. and Araya, K.** (2005). Phylogeny of Japanese stag beetles (Coleoptera: Lucanidae) inferred from 16S mtrRNA gene sequences, with reference to the evolution of sexual dimorphism of mandibles. *Zoolog. Sci.* **22**, 1305–1318.
- Inoue, A. and Hasegawa, E.** (2012). Effect of morph types, body size and prior residence on food-site holding by males of the male-dimorphic stag beetle *Prosopocoilus inclinatus* (Coleoptera: Lucanidae). *J. Ethol.* **31**, 55–60.
- Kawano, K.** (1997). Cost of evolving exaggerated mandibles in stag beetles (Coleoptera: Lucanidae). *Ann. Entomol. Soc. Am.* **90**, 453–461.
- Kawano, K.** (2000). Genera and allometry in the stag beetle family Lucanidae, Coleoptera. *Ann. Entomol. Soc. Am.* **93**, 198–207.
- Kim, S. I. and Farrell, B. D.** (2015). Phylogeny of world stag beetles (Coleoptera: Lucanidae) reveals a Gondwanan origin of Darwin's stag beetle. *Mol. Phylogenet. Evol.* **86**, 35–48.
- Klocke, D.** (2011). Water as a major modulator of the mechanical properties of insect cuticle. *Acta Biomater.* **7**, 2935–2942.
- Knell, R. J., Pomfret, J. C. and Tomkins, J. L.** (2004). The limits of elaboration: curved allometries reveal the constraints on mandible size in stag beetles. *Proc. R. Soc. B* **271**, 523–528.
- Knorr, E. M. and Ng, R. T.** (1997). A unified approach for mining outliers. *Proceedings of the 1997 conference of the Centre for Advanced Studies on Collaborative research*, 219–222.
- Lagarde, F., Corbin, J., Goujon, C. and Poisbleau, M.** (2005). Polymorphisme et performances au combat chez les mâles de Lucane cerf-volant (*Lucanus cervus*). *La Rev. d'écologie (Terre vie)* **60**, 127–137.
- Lundrigan, B.** (1996). Morphology of horns and fighting behavior in the Family Bovidae. *J. Mammal.* **77**, 462–475.
- Maas, S. A., Ellis, B. J., Ateshian, G. A. and Weiss, J. A.** (2012). FEBio: finite elements for biomechanics. *J. Biomech. Eng.* **134**, 011005.
- McCullough, E. L., Tobalske, B. W. and Emlen, D. J.** (2014). Structural adaptations to diverse fighting styles in sexually selected weapons. *Proc. Natl. Acad. Sci. USA* **111**, 14484–14488.
- Mills, M. R., Nemri, R. S., Carlson, E. A., Wilde, W., Gotoh, H., Lavine, L. C. and Swanson, B. O.** (2016). Functional mechanics of beetle mandibles: honest signaling in a sexually selected system. *J. Exp. Zool. A* **325**, 3–12.
- Moran, P. A. P.** (1971). Estimating structural and functional relationships. *J. Multivar. Anal.* **1**, 232–255.
- Okada, Y. and Hasegawa, E.** (2005). Size-dependent precopulatory behavior as mate-securing tactic in the Japanese stag beetle, *Prosopocoilus inclinatus* (Coleoptera; Lucanidae). *J. Ethol.* **23**, 99–102.
- Okada, K. and Miyatake, T.** (2006). Ownership-dependent mating tactics of minor males of the beetle *Librodor japonicus* (Nitidulidae) with intra-sexual dimorphism of mandibles. *J. Ethol.* **25**, 255–261.
- Percy, C.** (1998). *Findings of the 1998 National Stag Beetle Survey*. <http://ptes.org/wp-content/uploads/2014/06/Great-Stag-Hunt-1998.pdf>.
- Rayfield, E. J.** (2007). Finite element analysis and understanding the biomechanics and evolution. *Annu. Rev. Earth Planet. Sci.* **35**, 541–576.
- Ross, C. F., Patel, B. A., Slice, D. E., Strait, D. S., Dechow, P. C., Richmond, B. G. and Spencer, M. A.** (2005). Modeling masticatory muscle force in finite element analysis: sensitivity analysis using principal coordinates analysis. *Anat. Rec. A. Discov. Mol. Cell. Evol. Biol.* **283**, 288–299.
- Rowland, J. M. and Emlen, D. J.** (2009). Two thresholds, three male forms result in facultative male trimorphism in beetles. *Science*. **323**, 773–776.
- Shiokawa, T. and Iwahashi, O.** (2000). Mandible dimorphism in males of a stag beetle, *Prosopocoilus dissimilis okinawanus* (Coleoptera: Lucanidae). *Appl. Entomol. Zool.* **35**, 487–494.
- Smith, R. J.** (2009). Use and misuse of the reduced major axis for line-fitting. *Am. J. Phys. Anthropol.* **140**, 476–486.
- Soons, J., Genbrugge, A., Podos, J., Adriaens, D., Aerts, P., Dirckx, J. and Herrel, A.** (2015). Is beak morphology in Darwin's finches tuned to loading demands? *PLoS ONE* **10**, e0129479.
- Taylor, G.** (2000). Variation in safety factors of claws within and among six species of *Cancer* crabs (Decapoda: Brachyura). *Biol. J. Linn. Soc.* **70**, 37–62.
- Taylor, G. and Thomas, A.** (2014). *Evolutionary Biomechanics: Selection, Phylogeny, and Constraint*. Oxford: OUP.
- van der Meijden, A., Kleinteich, T. and Coelho, P.** (2012). Packing a pinch: functional implications of chela shapes in scorpions using finite element analysis. *J. Anat.* **220**, 423–434.
- Vincent, J. F. V. and Wegst, U. G. K.** (2004). Design and mechanical properties of insect cuticle. *Arthropod Struct. Dev.* **33**, 187–199.
- Wainwright, P. C., Alfaro, M. E., Bolnick, D. I. and Hulsey, C. D.** (2005). Many-to-one mapping of form to function: a general principle in organismal design? *Integr. Comp. Biol.* **45**, 256–262.
- Young, R. L., Haselkorn, T. S. and Badyaev, A. V.** (2007). Functional equivalence of morphologies enables morphological and ecological diversity. *Evolution* **61**, 2480–2492.